Research Article

Noncoherent Spectral Optical CDMA System Using 1D Active Weight Two-Code Keying Codes

Bih-Chyun Yeh

Department of Electrical Engineering, School of Electrical and Computer Engineering, College of Engineering,
Chang-Gung University, Tao-Yuan, Taiwan

Correspondence should be addressed to Bih-Chyun Yeh; bih.chyun.yeh@gmail.com

We propose a new family of one-dimensional (1D) active weight two-code keying (TCK) in spectral amplitude coding (SAC) optical code division multiple access (OCDMA) networks. We use encoding and decoding transfer functions to operate the 1D active weight TCK. The proposed structure includes an optical line terminal (OLT) and optical network units (ONUs) to produce the encoding and decoding codes of the proposed OLT and ONUs, respectively. The proposed ONU uses the modified cross-correlation to remove interferences from other simultaneous users, that is, the multiuser interference (MUI). When the phase-induced intensity noise (PIIN) is the most important noise, the modified cross-correlation suppresses the PIIN. In the numerical results, we find that the bit error rate (BER) for the proposed system using the 1D active weight TCK codes outperforms that for two other systems using the 1D M-Seq codes and 1D balanced incomplete block design (BIBD) codes. The effective source power for the proposed system can achieve −10 dBm, which has less power than that for the other systems.

1. Introduction

Optical code division multiple access (OCDMA) systems are used in various network applications and their performance has become crucial [1–4]. These systems have the potential to provide network control, enhanced information security, and improved spectral efficiency [5–8]. OCDMA systems use a passive optical network (PON), which requires optical components such as couplers, splitters, combiners, and switches, and use multiple access points to remove interferences in the code sequences that are caused by different users. Encoding/decoding approaches are used to construct OCDMA systems and suppress the multiuser interference (MUI) [9–11] that arises when using shared channels with the same frequency spectrum. In addition, the OCDMA systems use photodiodes to shield them from the effects of phase-induced intensity noise (PIIN) [12–16], a design feature of such systems.

Seyedzadeh et al. [17] reported experimental and simulation results from a variable-weight spectral amplitude coding optical code division multiple access (VW-SAC-OCDMA) system. The results outlined a back-to-back system

with a minimum average power per chip, which maintained acceptable performance. The transmission used 60 km of fiber. The VW-SAC-OCDMA system used a mathematical approximation to calculate its capacity. The experimental results showed the bit error rate (BER) in the channels. The system uses the VW-SAC-OCDMA as a potential solution for QoS differentiation and flexible structure in metro networks.

Mostafa et al. [18] proposed that the PIIN and MUI are the main parameters that affect the performance of OCDMA systems. They lead to degradations in system performance and a reduction in the number of active users. The authors presented a system with an efficiently modified multiservice (MMS) code to produce the encoding spectral amplitude of the optical source in OCDMA systems, which avoided the PIIN and MUI. The code disposed the effect of the MUI and PIIN and gave better performance than other traditional codes. Also, the system had a practical code length with a simple receiver structure. The design of the codes in the SAC-OCDMA system used a critical parameter to overcome the system's drawbacks. Yeh [19] proposed the 1D added length codes to add the code length. At the same time, the cross-correlation of the 1D added length codes eliminated the

MUI and suppressed the PIIN. The 1D added length codes produced the scheme using one-code keying.

In this paper, we propose a new family of new codes for OCDMA systems named 1D active weight two-code keying (TCK) codes. We use an encoding transfer function to transfer the information bits into the code sequences of the 1D active weight TCK codes and a decoding transfer function to transfer the code sequences into the recovered bits. The optical line terminal (OLT) of the proposed structure obtains the information bits used to produce the encoding codes, and the optical network units (ONUs) of the proposed structure obtain the code sequences used to produce the decoding codes. The proposed ONUs use the modified cross-correlation to calculate the recovered bits. Because the photodiodes suffer from interference from other simultaneous users (i.e., MUI), the modified cross-correlation removes this. The PIIN is the most prominent type of noise and is based on the number of simultaneous users; the proposed ONUs use the modified cross-correlation to suppress the PIIN. In the numerical results, with an effective source power of -10 dBm, a data transmission rate of 2.5 Gbps, and a BER of 10^{-9}, the number of simultaneous users for the proposed system is 30 users. The number of possible simultaneous users for the proposed system is larger than that for other systems, that is, those that use 1D M-Seq codes and 1D BIBD codes. The effective source power for the proposed system using the 1D active weight TCK codes is -10 dBm, which is lower power than that for the other systems.

The rest of the paper is organized as follows. The properties of the 1D active weight TCK codes are derived in Section 2. In Section 3, we describe the system architecture. In Section 4, we analyze the system performance using the photocurrents of the photodiodes to determine the signal to noise ratio (SNR) and the BER. In Section 5, we show the numerical results of the performance of the 1D active weight TCK codes. Finally, in Section 6, we provide summary and conclusions.

2. 1D Active Weight TCK Codes

We propose one-dimensional (1D) active weight TCK codes for use in spectral amplitude coding (SAC) OCDMA networks. In this paper, we introduce a code family to create the codes, which produces their code sequences. The codes use two-code keying to generate the code sequences, which are defined by the information bits "0" and "1." These code sequences are used by optical communication systems. The proposed codes generate a Galois field of GF(k), where k is a prime number. The codes have a weight of k and a length of $2k^2$, and an encoding transfer function is used to produce the code weight position. The code weight position is a function of the prime number k and is defined as follows:

$$S_{M,O,m}(p) = 2(p * M - k - O - r) \mod k + m - 1, \quad (1)$$

where k is a prime number with the Galois field GF(k), p is $[0, 1, \ldots, k-1]$, M is $[0, 1, \ldots, k-1]$, O is $[0, 1, \ldots, k-1]$, r is a fixed value in the range $[0, 1, \ldots, k-1]$, mod is the remainder calculation for the modulo operation, and m is $[1, 2]$. The code weight position is directly converted to $[0, 1, \ldots, 2k-1]$.

We use the code weight position to extend the code sequences $c_{M,O,m}(n)$ as follows:

$$c_{M,O,m}(n) = \begin{cases} 1, & \text{if } n = 2kp + S_{M,O,m}(p), \\ 0, & \text{else}, \end{cases} \quad (2)$$

where n is the input of $c_{M,O,m}(n)$ and $c_{M,O,m}(n)$ is the elements of the code sequence $C_{M,O,m}$ of the codes. Table 1 shows the codes derived using the prime number $k = 3$.

The proposed codes use the derived code sequences to operate the decoding transfer function, which produces a modified cross-correlation. The cross-correlation between the code sequences $C_{M,O,m}$ and $C_{M',O',m'}$ is expressed as follows:

$$C_{M,O,m} \odot C_{M',O',m'} = \sum_{n=0}^{2k^2-1} c_{M,O,m}(n) c_{M',O',m'}(n), \quad (3)$$

where the code sequences $C_{M,O,m}$ and $C_{M',O',m'}$ are both 1D active weight TCK codes, $\odot$ is the dot-product of two vectors, and $c_{M,O,m}(n)$ and $c_{M',O',m'}(n)$ are the elements of the code sequences $C_{M,O,m}$ and $C_{M',O',m'}$, respectively. The cross-correlation of the codes is expressed as follows:

$$C_{M,O,m} \odot C_{M',O',m'}$$
$$= \begin{cases} k, & M = M', \ O = O', \ m = m' \\ 0, & M = M', \ O \neq O', \ m = m' \text{ or } m \neq m' \\ 1, & M \neq M', \ m = m', \end{cases} \quad (4)$$

where k is the code weight. The OCDMA system uses the code sequences to create cross-correlations exactly equal to k, 0, and 1. As shown in equation (4), the cross-correlations of the 1D active weight TCK codes are k for $M = M'$, $O = O'$, $m = m'$, 0 for $M = M'$, $O \neq O'$, $m = m'$ or $m \neq m'$, and 1 for $M \neq M'$, $m = m'$; that is, the codes have an autocorrelation value of k and have cross-correlation values of 0 or 1. When the proposed codes use cross-correlation, this causes interference in the code sequences.

The code sequence of the 1D active weight TCK codes has the one-characteristic matrix $C_{M,O+1,m}$. We generate the code sequence $C_{M,O+1,m}$ to produce the cross-correlation between the code sequences $C_{M,O+1,m}$ and $C_{M',O',m'}$ as follows:

$$C_{M,O+1,m} \odot C_{M',O',m'}$$
$$= \begin{cases} k, & M = M', \ O + 1 = O', \ m = m' \\ 0, & M = M', \ O + 1 \neq O', \ m = m' \text{ or } m \neq m' \\ 1, & M \neq M', \ m = m'. \end{cases} \quad (5)$$

Thus, $M = M'$, $O + 1 = O'$, and $m = m'$ produce a cross-correlation $= k$, $M = M'$, $O + 1 \neq O'$, $m = m'$, and $m \neq m'$ produce a cross-correlation $= 0$, and $M \neq M'$, $m = m'$ produce a cross-correlation $= 1$. We use $C_{M,O,m} \odot$

TABLE 1: Code sequences of the 1D active weight TCK codes with $k = 3$.

Code sequences of the 1D active weight TCK codes																	
0	0	0	0	1	0	0	0	0	0	1	0	0	0	0	0	1	0
0	0	1	0	0	0	0	0	1	0	0	0	0	0	1	0	0	0
1	0	0	0	0	0	1	0	0	0	0	0	1	0	0	0	0	0
0	0	0	0	1	0	1	0	0	0	0	0	0	0	1	0	0	0
0	0	1	0	0	0	0	0	0	0	1	0	1	0	0	0	0	0
1	0	0	0	0	0	0	0	1	0	0	0	0	0	0	0	1	0
0	0	0	0	1	0	0	0	1	0	0	0	1	0	0	0	0	0
0	0	1	0	0	0	1	0	0	0	0	0	0	0	0	0	1	0
1	0	0	0	0	0	0	0	0	0	1	0	0	0	1	0	0	0
0	0	0	0	0	1	0	0	0	0	0	1	0	0	0	0	0	1
0	0	0	1	0	0	0	0	0	1	0	0	0	0	0	1	0	0
0	1	0	0	0	0	0	1	0	0	0	0	0	1	0	0	0	0
0	0	0	0	0	1	0	1	0	0	0	0	0	0	0	1	0	0
0	0	0	1	0	0	0	0	0	0	0	1	0	1	0	0	0	0
0	1	0	0	0	0	0	0	0	1	0	0	0	0	0	0	0	1
0	0	0	0	0	1	0	0	0	1	0	0	0	1	0	0	0	0
0	0	0	1	0	0	0	1	0	0	0	0	0	0	0	0	0	1
0	1	0	0	0	0	0	0	0	0	0	1	0	0	0	1	0	0

$C_{M',O',m'}$ and $C_{M,O+1,m} \odot C_{M',O',m'}$ to produce the modified cross-correlation using the following transformation:

$$C_{M,O,m} \odot C_{M',O',m'} - C_{M,O+1,m} \odot C_{M',O',m'}$$

$$= \begin{cases} k, & M = M', \ O = O', \ m = m', \\ -k, & M = M', \ O + 1 = O', \ m = m', \\ 0, & \text{otherwise,} \end{cases} \quad (6)$$

where the values of the modified cross-correlation are the ideal cross-correlation with k, $-k$, and 0, respectively. Furthermore, we subtract $C_{M,O+1,m} \odot C_{M',O',m'}$ from $C_{M,O,m} \odot C_{M',O',m'}$ to produce the modified cross-correlation. The proposed codes use the modified cross-correlation = k for $M = M'$, $O = O'$, $m = m'$ to produce the code sequence $C_{M,O,m}$ from the recovered "0" bits. Similarly, the proposed codes use the modified cross-correlation = $-k$ for $M = M'$, $O + 1 = O'$, $m = m'$ to produce the code sequence $C_{M,O+1,m}$ from the recovered "1" bits. The proposed codes use the modified cross-correlation = 0 otherwise. Therefore, the proposed codes produce the code sequences $C_{M,O,m}$ and $C_{M,O+1,m}$, which are the recovered "0" and "1" bits, respectively.

First, cardinality comparison, the 1D active weight TCK codes get the code length equal to code size to produce the better cardinality. Then, the 1D MDW codes proposed by Aljunid et al. [20] used the code length to reduce the code size, which made the cardinality loss. The cardinality of the 1D active weight TCK codes is better than that of the 1D MDW codes.

Second, in autocorrelation and cross-correlation comparison, we find the 1D MDW codes with the one-code key (OCK) to get the autocorrelation and cross-correlation [20]. The 1D MDW codes get the cross-correlation of the 1D MDW codes to produce the OCK. In fact, the comparison between and 1D active weight TCK codes and 1D MDW codes with the OCK is dependent on the cross-correlation. The 1D active weight TCK codes transfer the information bit = "1" and "0" into the code sequence with the information bit "1" and code sequence with the information bit "0," which get "k" of the cross-correlation in the receiver and "$-k$" of the cross-correlation in the receiver to combine the level "0" of the cross-correlation in the receiver. The 1D MDW codes transfer the information bit = "1" and "0" into the code sequence with the information bit "1" and no code sequence, which get "k" of the cross-correlation in the receiver and "0" of the cross-correlation in the receiver to combine the level "$k/2$" of the cross-correlation in the receiver. The level of the cross-correlation in the receiver in the 1D active weight TCK codes shows better performance than that in the 1D MDW codes.

We get the first cardinality comparison and second autocorrelation and cross-correlation comparison to operate the method comparison. The method comparison of the 1D active weight TCK codes is better than that of the 1D MDW codes.

Furthermore, when the code sequences $C_{M,O,m}$ and $C_{M,O+1,m}$ are assigned to the same user for two-code keying, we use a MUI elimination scheme to solve the problem of interference from other simultaneous users using the modified cross-correlation. When we use the 1D active weight TCK codes to produce the modified cross-correlation, the modified cross-correlation produces a recovered "0" or "1" bit. Moreover, photodiodes using the modified cross-correlation suppress the PIIN. Therefore, the proposed codes
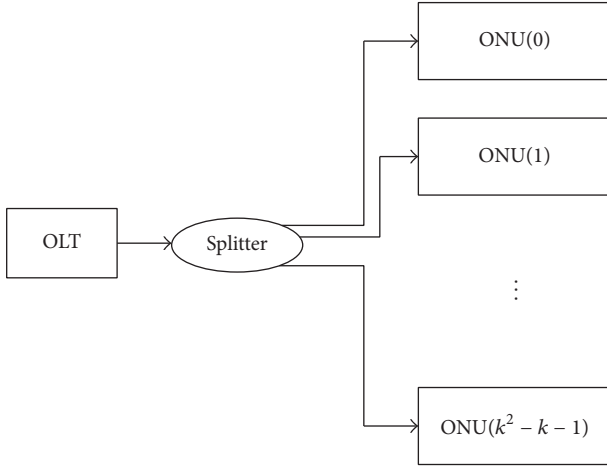
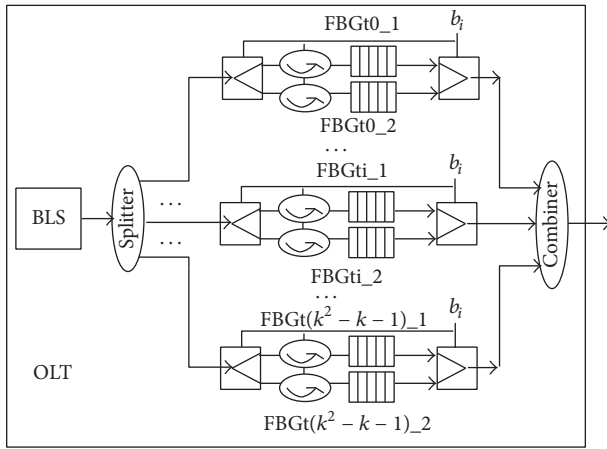FIGURE 1: Schematic block diagram of the 1D active weight TCK codes.

FIGURE 2: The structure of the OLT.

use the modified cross-correlation to remove MUI and suppress the PIIN.

3. System Description

Figure 1 shows the schematic block diagram of the 1D active weight TCK codes. The proposed structure of the OCDMA system comprises the OLT, a $(k^2 - k)$ optical splitter, and $(k^2 - k)$ ONUs. The optical signals using the code sequences are sent from the OLT to the optical splitter, which connects to the ONUs. The optical splitter sends the code sequences into the ONUs, each of which recovers the appropriate bits from the code sequences. We use the proposed structure of the OCDMA system to develop the OLT, the optical splitter, and the ONUs.

Figure 2 shows the proposed structure of the OLT, which comprises an unpolarized broadband light source (BLS), a $(k^2 - k)$ optical splitter, $(k^2 - k) 1 \times 2$ optical switches with controlled value $b_i, i = 0, 1, \ldots, (k^2 - k) - 1, 2 * (k^2 - k)$ optical circulators, $2 * (k^2 - k)$ fiber Bragg gratings, $(k^2 - k) 2 \times 1$ optical
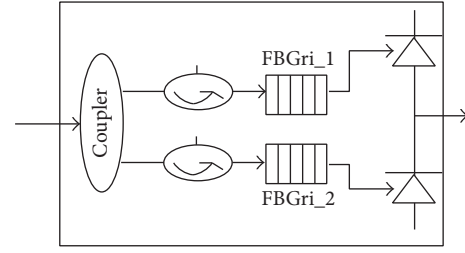

FIGURE 3: The structure of the ONU(i).

switches with controlled value $b_i, i = 0, 1, \ldots, (k^2 - k) - 1$, and a $(k^2 - k) \times 1$ optical combiner. The unpolarized BLS connects to the optical splitter, which connects to the 1×2 optical switches. These switches then connect to the optical circulators, which connect to the fiber Bragg gratings and then to the 2×1 optical switches. Finally, these switches connect to the optical combiner.

The unpolarized BLS emits light, which passes through the optical splitter and is controlled by the value b_i. If the information bit $b_i = 0$, the light is switched to the optical circulator and fiber Bragg grating FBGti_1. The optical signal then goes through the 2×1 switch with the control value $b_i = 0$. If the information bit $b_i = 1$, the light is switched to the optical circulator and fiber Bragg grating FBGti_2, and the optical signal goes through the 2×1 switch with the control value $b_i = 1$.

The fiber Bragg grating FBGti_1 corresponds to the complementary code sequence $C_{M,O,m}$ of the 1D active weight TCK codes; it allows the code sequence $C_{M,O,m}$ through and filters out the complementary code sequence $\overline{C_{M,O,m}}$. Similarly, the FBGti_2 grating corresponds to the complementary code sequence $C_{M,O+1,m}$; it allows the code sequence $C_{M,O+1,m}$ through and filters out the complementary code sequence $\overline{C_{M,O+1,m}}$.

We use the control value b_i to allow either the fiber Bragg grating FBGti_1 or the fiber Bragg grating FBGti_2 to connect to the 2×1 optical switches. The light passing through these switches is combined by the optical combiner. Therefore, we use the information bit $b_i = 0$ or bit $b_i = 1$ to divert the light into either FBGti_1 or FBGti_2, which outputs code sequences with information bit 0 or information bit 1, respectively.

Figure 3 shows the proposed structure of the ONU(i), $i = [0, 1, \ldots, (k^2 - k) - 1]$. The structure comprises a 1×2 optical coupler, an upper optical circulator, a lower optical circulator, a fiber Bragg grating FBGri_1, a fiber Bragg grating FBGri_2, and a balanced detector between the upper and lower photodiodes. The code sequences of the 1D active weight TCK codes connect to the optical coupler, which connects to the upper and lower optical circulators. The upper and lower optical circulators connect to the fiber Bragg gratings FBGri_1 and FBGri_2, respectively, which then connect to the upper and lower photodiodes.

The code sequences pass through the upper optical circulator to the fiber Bragg grating FBGri_1, which corresponds to the complementary code sequence $C_{M,O,m}$. The grating FBGri_1 allows the code sequence $C_{M,O,m}$ through and filters out the complementary code sequence

$C_{M,O,m}$. Similarly, in the lower optical circulator, the FBGri_2 grating allows $C_{M,O+1,m}$ code sequence through and filters out the complementary code sequence $C_{M,O+1,m}$. Thus, we use the fiber Bragg gratings FBGri_1 and FBGri_2 to send data to the upper and lower photodiodes of the balanced detector. The modified cross-correlation allows the balanced detector to obtain a recovered "0" or "1" bit.

The output photocurrent of photodiode PD0 is proportional to $C_{M,O,m} \odot C_{M',O',m'}$, and that of photodiode PD1 is proportional to $C_{M',O+1,m} \odot C_{M',O',m'}$. As the proposed system can be described by (6), the modified photocurrent of the modified cross-correlation is proportional to $C_{M,O,m} \odot C_{M',O',m'} - C_{M,O+1,m} \odot C_{M',O',m'}$, which is k for $M = M'$, $O = O'$, $m = m'$, $-k$ for $M = M'$, $O + 1 = O'$, $m = m'$, or 0 otherwise. Because the MUI is produced by the interferences from other simultaneous users using unmatched code words, we can use the modified cross-correlation to completely eliminate it. Moreover, because the PIIN is based on the noise in the photodiodes, it is suppressed by the photocurrent arising from the modified cross-correlation.

4. Performance Analysis

To analyze performance, we used the optical signal and various noise parameters to determine the SNR and BER. The optical signal is measured from the photocurrent produced by the photodiodes. The noises arise from the PIIN, shot noise, and thermal noise and change the photocurrent noise variances accordingly. The SNR is created by dividing the modified photocurrent of the optical signal by the photocurrent noises variances in the photodiodes. The BER uses the Gaussian approximation to calculate the SNR. Therefore, we can obtain the BER of the 1D active weight TCK codes to observe their performance.

The ONU receives the code sequences of the 1D active weight TCK codes, and we use the optical signals to produce the PSD of the received optical signals. The PSD of the received optical laser signals in the ONU(i) can be set as follows:

$$R(f) = \frac{P_{\text{sr}}}{\Delta f} \int_0^\infty \sum_{p=1}^{P} \Lambda(p) \\ \cdot \sum_{M'=0}^{k-1} \sum_{O'=0}^{k-1} \sum_{m'=1}^{2} \sum_{q=0}^{2k^2-1} (c_{M',O',m'}(q)) F(f,q) \, df, \tag{7}$$

where P_{sr} is the effective source power at the ONU(i), Δf is the bandwidth of the source, $\Lambda(p)$ is the recovered bit of the pth user, which can be 0 or 1, P is the number of simultaneous users, k is the code weight, $c_{M',O',m'}$ is an element of the pth user's code sequence, and $F(f,q)$ is the wavelength chip. For the convenience of analysis, the proposed system defines $F(f,q)$ to be as follows:

$$F(f,q) = \left\{ \Theta\left(f - f_o - \frac{\Delta f\left(-\left(2k^2\right) + 2q\right)/2}{\left(2k^2\right)} \right) \\ - \Theta\left(f - f_o - \frac{\Delta f\left(-\left(2k^2\right) + 2q + 2\right)/2}{\left(2k^2\right)} \right) \right\}. \tag{8}$$

The unit step function $\Theta(f)$ is as follows:

$$\Theta(f) = \begin{cases} 1, & f \geq 0, \\ 0, & f < 0. \end{cases} \tag{9}$$

Therefore, the PSDs of the received optical signals show the power required using the code sequences to arrive at the ONUs. Based on this simplified analysis, some assumptions follow. The proposed system assumes each of the spectral components to have identical spectral width. The broadband light source is ideally unpolarized and has a flat spectrum over $[f_o - \Delta f/2, f_o + \Delta f/2]$, where f_o and Δf are the central frequency and bandwidth of the source. The proposed system thus has equal power at the ONUs.

The ONU computes a cross-correlation between the code sequences $c_{M,O,m}$ and $c_{M',O',m'}$ and between the code sequences $c_{M,O+1,m}$ and $c_{M',O',m'}$. The PSDs at the photodiodes using the cross-correlations during a one-bit period can be described as follows:

$$X_0(f) = \frac{P_{\text{sr}}}{\Delta f} \int_0^\infty \sum_{p=1}^{P} \Lambda(p) \\ \cdot \sum_{M'=0}^{k-1} \sum_{O'=0}^{k-1} \sum_{m'=1}^{2} \sum_{q=0}^{2k^2-1} (c_{M,O,m}(q)\, c_{M',O',m'}(q)) F(f,q) \, df, \\ X_1(f) = \frac{P_{\text{sr}}}{\Delta f} \int_0^\infty \sum_{p=1}^{P} \Lambda(p) \\ \cdot \sum_{M'=0}^{k-1} \sum_{O'=0}^{k-1} \sum_{m'=1}^{2} \sum_{q=0}^{2k^2-1} (c_{M,O+1,m}(q)\, c_{M',O',m'}(q)) F(f,q) \, df, \tag{10}$$

where k is the code weight of the code sequence. In addition, the proposed system uses $\Lambda(p) = 1$ and $p = 1, 2, \ldots, P$ in the worst case, as well as the cross-correlations, to determine the maximum interferences produced by the other simultaneous users, known as the MUI. For the photodiodes PD0 and PD1, the photocurrents I_{PD0} and I_{PD1} are described as follows:

$$I_{\text{PD0}} = R \int_0^\infty X_0(f) \, df = R \frac{P_{\text{sr}}}{\Delta f} \int_0^\infty \sum_{p=1}^{P} \Lambda(p) \\ \cdot \sum_{M'=0}^{k-1} \sum_{O'=0}^{k-1} \sum_{m'=1}^{2} \sum_{q=0}^{2k^2-1} (c_{M,O,m}(q)\, c_{M',O',m'}(q)) F(f,q) \, df \\ = R \frac{P_{\text{sr}}}{2k^2} \left(k + \frac{(P-1)*\left(k^2 - 2k + 1\right)}{2k^2 - 2k - 1} \right), \\ I_{\text{PD1}} = R \int_0^\infty X_1(f) \, df = R \frac{P_{\text{sr}}}{\Delta f} \int_0^\infty \sum_{p=1}^{P} \Lambda(p) \\ \cdot \sum_{M'=0}^{k-1} \sum_{O'=0}^{k-1} \sum_{m'=1}^{2} \sum_{q=0}^{2k^2-1} (c_{M,O+1,m}(q)\, c_{M',O',m'}(q)) F(f,q) \, df \\ = R \frac{P_{\text{sr}}}{2k^2} \left(\frac{(P-1)*\left(k^2 - 2k + 1\right)}{2k^2 - 2k - 1} \right), \tag{11}$$

where G is the average gain, R is the responsivity of the photodiode given by $R = \eta e \lambda_o / hc$, η is the quantum efficiency of the photodiode, e is the charge on the electron, λ_o is a central wavelength, h is Planck's constant, c is the speed of light, and P_{sr} is the effective source power of each ONU. Therefore, the proposed system forces the photocurrents of the photodiodes PD0 and PD1 to be proportional to the cross-correlations and uses the cross-correlations to produce a modified photocurrent. The modified photocurrent can be written as

$$I_{m,\text{bit}=0} = R \int_0^\infty [X_0(f) - X_1(f)] \, df = (I_{PD0} - I_{PD1})$$

$$= R \frac{P_{sr}}{2k}. \tag{12}$$

$$I_{m,\text{bit}=1} = (I_{PD0} - I_{PD1}) = -R \frac{P_{sr}}{2k}.$$

Therefore, the proposed system uses the modified cross-correlation to produce a modified photocurrent, removing the MUI.

The noise variances in the modified photocurrent have various effects on system performance. The photocurrent noise variances are as follows:

$$\langle i_{\text{noise}}^2 \rangle = \langle i_{\text{PIIN,bit}=\times}^2 \rangle + \langle i_{\text{shot,bit}=\times}^2 \rangle + \langle i_{\text{thermal}}^2 \rangle$$

$$= I_{m,\text{bit}=\times}^2 B_r \tau + 2e I_{t,\text{bit}=\times} B_r + \frac{4 K_a T_n B_r}{R_o}, \tag{13}$$

where bit $= x$ is from the "0" or "1", PIIN, shot noise, and thermal noise are considered in the photocurrent analysis, the effect of the dark current is neglected, $I_{m,\text{bit}=\times}$ is the modified photocurrent, $I_{t,\text{bit}=\times}$ is the total photocurrent, B_r is the electrical bandwidth, τ is the coherence time of the light incident to the photodiode, e is the charge on the electron, K_a is Boltzmann's constant, T_n is the absolute noise temperature, and R_o is the load resistance. Therefore, τ can be described as follows:

$$\tau = \frac{\int_0^\infty X^2(f) \, df}{\left[\int_0^\infty X(f) \, df\right]^2}, \tag{14}$$

where $X(f)$ is the single sideband power spectral density (PSD) of the light incident on the photodiodes. The photocurrent noise variances are based on statistically independent noise characteristics, because the PIIN, shot noise, and thermal noise are independent noises. Therefore, the PIIN, shot noise, and thermal noise all cause independent variance in the photocurrent and thus have independent influences on system performance.

The photocurrent PIIN variance is shown in (13) and is defined as follows:

$$\langle i_{\text{PIIN,bit}=0}^2 \rangle = B_r I_{m,\text{bit}=0}^2 \tau, \tag{15}$$

where B_r denotes the electrical bandwidth and τ is the coherence time of the light incident on the photodiode. When the spectrum of $X_0(f)$ does not overlap the spectrum of

$X_1(f)$, the photocurrent PIIN variance of the ONU can be written as

$$\langle i_{\text{PIIN,bit}=0}^2 \rangle = B_r I_{m,\text{bit}=0}^2 \frac{\int_0^\infty [X_0(f) - X_1(f)]^2 \, df}{\left\{\int_0^\infty [X_0(f) - X_1(f)] \, df\right\}^2}$$

$$= B_r R^2 \int_0^\infty [X_0(f) - X_1(f)]^2 \, df$$

$$= B_r R^2 \int_0^\infty [X_0(f)]^2 + [X_1(f)]^2 \tag{16}$$

$$- 2 X_0(f) X_1(f) \, df = B_r R^2 \int_0^\infty [X_0(f)]^2$$

$$+ [X_1(f)]^2 \, df.$$

When the proposed system produces $X_t(f)$, $t = [0,1]$ as in (10), we have $X_t^2(f)$, $t = [0,1]$ as follows:

$$\int_0^\infty X_0^2(f) \, df = \frac{P_{sr}^2}{\Delta f^2} \int_0^\infty \left[\sum_{p=1}^{P} \Lambda(p) \right.$$

$$\left. \cdot \sum_{M'=0}^{k-1} \sum_{O'=0}^{k-1} \sum_{m'=1}^{2} \sum_{q=0}^{2k^2-1} (c_{M,O,m}(q) \, c_{M',O',m'}(q)) F(f,q) \right]^2 \, df$$

$$= \frac{P_{sr}^2}{2k^2 \Delta f} \sum_{q=0}^{2k^2-1} \left[\sum_{p=1}^{P} \Lambda(p) \right.$$

$$\left. \cdot \sum_{M'=0}^{k-1} \sum_{O'=0}^{k-1} \sum_{m'=1}^{2} (c_{M,O,m}(q) \, c_{M',O',m'}(q)) F(f,q) \right]^2$$

$$= \frac{P_{sr}^2}{\Delta f * 2k^3} \left[k + \frac{(P-1)*(k-1)*k}{2k^2 - 2k - 1} \right]^2,$$

$$\int_0^\infty X_1^2(f) \, df = \frac{P_{sr}^2}{\Delta f^2} \int_0^\infty \left[\sum_{p=1}^{P} \Lambda(p) \right. \tag{17}$$

$$\left. \cdot \sum_{M'=0}^{k-1} \sum_{O'=0}^{k-1} \sum_{m'=1}^{2} \sum_{q=0}^{2k^2-1} (c_{M,O+1,m}(q) \, c_{M',O',m'}(q)) F(f,q) \right]^2 \, df$$

$$= \frac{P_{sr}^2}{2k^2 \Delta f} \sum_{q=0}^{2k^2-1} \left[\sum_{p=1}^{P} \Lambda(p) \right.$$

$$\left. \cdot \sum_{M'=0}^{k-1} \sum_{O'=0}^{k-1} \sum_{m'=1}^{2} (c_{M,O+1,m}(q) \, c_{M',O',m'}(q)) F(f,q) \right]^2$$

$$= \frac{P_{sr}^2}{\Delta f * 2k^3} \left[\frac{(P-1)*(k-1)*k}{2k^2 - 2k - 1} \right]^2.$$

The PIIN has the most important effect on system performance. By substituting (17) into (16), the PIIN can be expressed as follows:

$$
\left\langle i_{\text{PIIN,bit=0}}^2 \right\rangle
$$

$$
= \frac{P_{\text{sr}}^2}{\Delta f * 2k^3} \left\{ \left[k + \frac{(P-1)*(k-1)*k}{2k^2 - 2k - 1} \right]^2 \right. \tag{18}
$$

$$
\left. + \left[\frac{(P-1)*(k-1)*k}{2k^2 - 2k - 1} \right]^2 \right\}.
$$

The proposed system uses the modified cross-correlation to produce a recovered bit with a value of 0 or 1. Every simultaneous user produces a 0 or a 1, which are sent with equal probability. The value of $\langle i_{\text{PIIN,bit=1}}^2 \rangle$ is equal to that of $\langle i_{\text{PIIN,bit=0}}^2 \rangle$, so the PIIN influences the performance of the proposed system.

The shot noise also influences the photocurrent variance, and the photocurrent shot noise variance can be described as

$$
\left\langle i_{\text{shot,bit=0}}^2 \right\rangle = 2eB_r I_{t,\text{bit=0}}, \tag{19}
$$

where $I_{t,\text{bit=0}}$ is the total photocurrent according to $I_{t,\text{bit=0}} = I_{\text{PD0}} + I_{\text{PD1}}$. The recovered 0 and 1 bits are sent with equal probability for every simultaneous user. The value of $\langle i_{\text{shot,bit=1}}^2 \rangle$ is equal to that of $\langle i_{\text{shot,bit=0}}^2 \rangle$. Therefore, the influence of the shot noise on system performance depends on the electronic charge and the total photocurrent.

The thermal noise arises from the effect of absolute temperature and load resistance, and the photocurrent thermal noise variance is described as follows:

$$
\left\langle i_{\text{thermal}}^2 \right\rangle = \frac{4K_a T_n B_r}{R_L}, \tag{20}
$$

where K_a is Boltzmann's constant, T_n is the absolute temperature, and R_L is the load resistance.

The SNR divides the square of the modified photocurrent by the photocurrent noise variances to produce the communication ability of the proposed system. Thus, the SNR is described as follows:

$$
\text{SNR}_{\text{bit=×}} = \frac{I_{m,\text{bit=×}}^2}{\langle i_{\text{noise}}^2 \rangle}
$$

$$
= \frac{I_{m,\text{bit=×}}^2}{\left(\langle i_{\text{PIIN,bit=×}}^2 \rangle + \langle i_{\text{shot,bit=×}}^2 \rangle + \langle i_{\text{thermal}}^2 \rangle \right)}. \tag{21}
$$

Because the BER uses the Gaussian approximation, it can be used to calculate the SNR. The BER can be expressed as

$$
\text{BER} = \frac{\text{erfc} \left(\sqrt{(\text{SNR}_{\text{bit=0}} \text{ or } \text{SNR}_{\text{bit=1}})/2} \right)}{2}, \tag{22}
$$

where erfc(·) is the complementary error function as follows:

$$
\text{erfc}(t) = \frac{2}{\sqrt{\pi}} \int_t^\infty \exp\left(-e^2\right) de. \tag{23}
$$

TABLE 2: Parameters used in the numerical calculation.

PD quantum efficiency	$\eta = 0.6$
Wavelength location	$\lambda = 1.55\,\mu m$
Data transmission rate	2.5 Gbps
Receiver noise temperature	$T_n = 300\,K$
Receiver load resistor	$R_L = 1030\,\Omega$

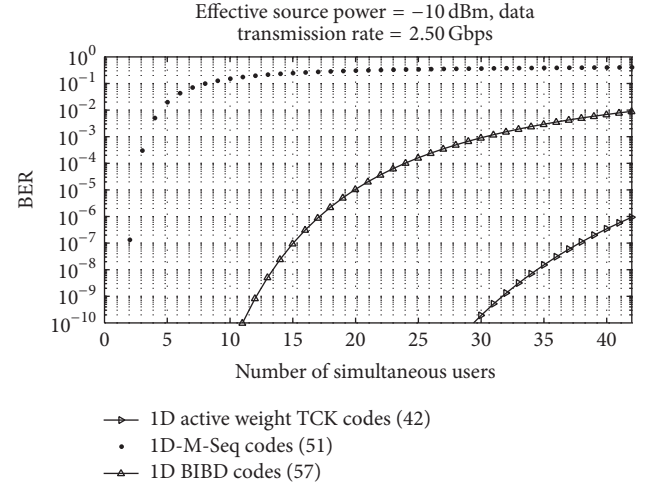FIGURE 4: The number of simultaneous users versus BER for the SAC-OCDMA systems using 1D active weight TCK codes, 1D M-Seq codes, and 1D BIBD codes.

5. Numerical Results

Table 2 shows the parameters used in the numerical calculation. The parameters consist of the PD quantum efficiency η, spectral width of broadband light source $\Delta\lambda$, wavelength location, data transmission rate, receiver noise temperature T_n, and receiver load resistor R_L. The parameters are calculated from the numerical results. Figure 4 shows the number of simultaneous users versus BER for the SAC-OCDMA systems using 1D active weight TCK codes, 1D M-Seq codes, and 1D BIBD codes. The proposed system and the other systems have similar code lengths. If we set the effective source power of all the systems to −10 dBm, their data transmission rates to 2.5 Gbps, and their BERs to 10^{-9}, we obtain 30 simultaneous users for the proposed system, one for the 1D M-Seq code system, and 11 for the 1D BIBD code system. The number of simultaneous users for the proposed system is larger, which improves its performance, making it superior to the other systems. Similarly, if we set effective source power to −10 dBm, data transmission rate to 2.5 Gbps, and number of simultaneous users to 30, the BER for the proposed system is 10^{-9}, that for the 1D M-Seq code system is $10^{-0.5}$, and that for the 1D BIBD code system is 10^{-3}. Thus, the BER for the proposed system is lower than that for the other systems.

Figure 5 shows the data transmission rate versus BER for the SAC-OCDMA systems using 1D active weight TCK codes, 1D M-Seq codes, and 1D BIBD codes. From Figure 5, when the number of simultaneous users is 30, the effective source power is −10 dBm, and the BER is 10^{-9}, the data
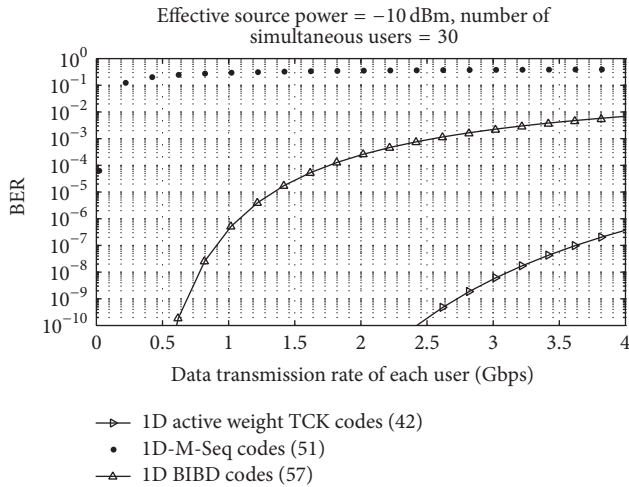
Figure 5: The data transmission rate versus BER for the SAC-OCDMA systems using 1D active weight TCK codes, 1D M-Seq codes, and 1D BIBD codes.
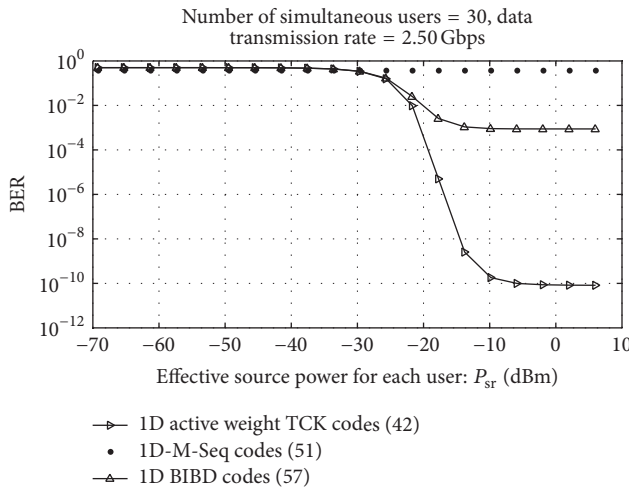

Figure 6: The effective source power versus BER for the SAC-OCDMA systems using 1D active weight TCK codes, 1D M-Seq codes, and 1D BIBD codes.

transmission rate for the proposed system is 2.5 Gbps, that for the 1D M-Seq code system is 0.01 Gbps, and that for the 1D BIBD code system is 0.74 Gbps. Thus, the data transmission rate for the proposed system is larger than that for the other systems, resulting in improved performance. When the number of simultaneous users is 30, the effective source power is −10 dBm, and the data transmission rate is 2.5 Gbps, the BER for the proposed system is 10^{-9}, that for the 1D M-Seq code system is $10^{-0.5}$, and that for the 1D BIBD code system is 10^{-3}. Thus, the BER for the proposed system is lower than that for the other systems.

Figure 6 shows the effective source power versus BER for the SAC-OCDMA systems using 1D active weight TCK codes, 1D M-Seq codes, and 1D BIBD codes. We set the number of simultaneous users to 30 users, data transmission rate to 2.5 Gbps, and BER to 10^{-9}. The effective source power

for the proposed system is −10 dBm and that for the other systems shows no crossing points. Thus, the effective source power for the proposed system is lower than that for the other systems. Finally, we set the number of simultaneous users to 30, the data transmission rate to 2.5 Gbps, and the effective source power to −10 dBm. The BER for the proposed system is 10^{-9}, that for the 1D M-Seq code system is $10^{-0.5}$, and that for the 1D BIBD code system is 10^{-3}. Thus, the BER for the proposed system is lower than that for the other systems.

6. Conclusions

In this paper, we proposed a new family of codes for OCDMA systems named 1D active weight TCK codes. We used encoding and decoding transfer functions to produce the 1D active weight two-code keying. The proposed structure includes an optical line terminal (OLT) and optical network units (ONUs) to produce the encoding and decoding codes of the proposed OLT and ONUs, respectively. The proposed ONU uses the modified cross-correlation to calculate the recovered bits. The modified cross-correlation removes the interferences from the other simultaneous users, the MUI. The influence of the PIIN, which is noise based on the number of simultaneous users, is reduced because the proposed ONUs use the modified cross-correlation to suppress it. In the numerical results, with an effective source power of −10 dBm, a data transmission rate of 2.5 Gbps, and a BER of 10^{-9}, the number of simultaneous users for the proposed system using 1D active weight TCK codes is 30, which is larger than that for other systems using 1D M-Seq codes and 1D BIBD codes. The effective source power for the proposed system using the 1D active weight TCK codes is −10 dBm, which is less power than that for the other systems.

Competing Interests

The author declares no competing interests.

Acknowledgments

References

[1] I. B. Djordjevic, B. Vasic, and J. Rorison, "Multi-weight unipolar codes for multimedia spectral-amplitude-coding optical CDMA systems," *IEEE Communications Letters*, vol. 8, no. 4, pp. 259–261, 2004.

[2] L. D. H. Sampaio, T. Abrão, B. A. Angélico, M. Lima, M. L. Proença Jr., and P. J. E. Jeszensky, "Hybrid heuristic-waterfilling game theory approach in MC-CDMA resource allocation," *Applied Soft Computing Journal*, vol. 12, no. 7, pp. 1902–1912, 2012.

[3] D. Kilper, K. Bergman, V. W. S. Chan, I. Monga, G. Porter, and K. Rauschenbach, "Optical networks come of age," *Optics and Photonics News*, vol. 25, no. 9, pp. 50–57, 2014.

[4] W. C. Kwong, P. A. Perrier, and P. R. Prucnal, "Performance comparison of asynchronous and synchronous code-division multiple-access techniques for fiber-optic local area networks," *IEEE Transactions on Communications*, vol. 39, no. 11, pp. 1625–1634, 1991.

[5] D. E. Leaird, Z. Jiang, and A. M. Weiner, "Experimental investigation of security issues in OCDMA: a code-switching scheme," *Electronics Letters*, vol. 41, no. 14, pp. 817–819, 2005.

[6] F. R. Durand, M. L. F. Abbade, F. R. Barbosa, and E. Moschim, "Design of multi-rate optical code paths considering polarisation mode dispersion limitations," *IET Communications*, vol. 4, no. 2, pp. 234–239, 2010.

[7] S. Singh, R. Kaur, A. Singh, and R. S. Kaler, "Novel security enhancement technique against eavesdropper for OCDMA system using 2-D modulation format with code switching scheme," *Optical Fiber Technology*, vol. 22, pp. 84–89, 2015.

[8] Z. Jiang, D. S. Seo, S.-D. Yang et al., "Four-user, 2.5-Gb/s, spectrally coded OCDMA system demonstration using low-power nonlinear processing," *Journal of Lightwave Technology*, vol. 23, no. 1, pp. 143–158, 2005.

[9] J.-F. Huang, K.-S. Chen, Y.-C. Lin, and C.-Y. Li, "Reconfiguring waveguide-gratings-based M-signature codecs to enhance OCDMA network confidentiality," *Optics Communications*, vol. 313, pp. 223–230, 2014.

[10] M. S. Anuar, S. A. Aljunid, N. M. Saad, and S. M. Hamzah, "New design of spectral amplitude coding in OCDMA with zero cross-correlation," *Optics Communications*, vol. 282, no. 14, pp. 2659–2664, 2009.

[11] T. R. Raddo, A. L. Sanches, J. V. dos Reis Jr., and B.-H. V. Borges, "A new approach for evaluating the BER of a multirate, multi-class OFFH-CDMA system," *IEEE Communications Letters*, vol. 16, no. 2, pp. 259–261, 2012.

[12] V. Jyoti and R. S. Kaler, "Novel anti-jamming technique for OCDMA network through FWM in SOA based wavelength converter," *Optical Fiber Technology*, vol. 19, no. 3, pp. 259–263, 2013.

[13] A. J. Dos Santos, F. R. Durand, and T. Abrao, "Mitigation of environmental temperature variation effects in OCDMA networks using PSO power control," *Journal of Optical Communications and Networking*, vol. 7, no. 8, Article ID 7184838, pp. 707–717, 2015.

[14] F. R. Durand, M. S. Filho, and T. Abrão, "The effects of power control on the optical CDMA random access protocol," *Optical Switching and Networking*, vol. 9, no. 1, pp. 52–60, 2012.

[15] M. Tang, C. Long, and X. Guan, "Nonconvex optimization for power control in wireless CDMA networks," *Wireless Personal Communications*, vol. 58, no. 4, pp. 851–865, 2011.

[16] M. Noshad and K. Jamshidi, "Bounds for the BER of codes with fixed cross correlation in SAC-OCDMA systems," *Journal of Lightwave Technology*, vol. 29, no. 13, Article ID 5763717, pp. 1944–1950, 2011.

[17] S. Seyedzadeh, G. A. Mahdiraji, R. K. Z. Sahbudin, A. F. Abas, and S. B. A. Anas, "Experimental demonstration of variable weight SAC-OCDMA system for QoS differentiation," *Optical Fiber Technology*, vol. 20, no. 5, pp. 495–500, 2014.

[18] S. Mostafa, A. E. N. A. Mohamed, F. E. A. El-Samie, and A. N. Z. Rashed, "Eradication of multiple access interference using a modified multi-service code for SAC–OCDMA," *Wireless Personal Communications*, vol. 83, no. 2, pp. 855–872, 2015.

[19] B.-C. Yeh, "Noncoherent spectral optical code division multiple access system using one-dimensional added length codes," *Optical and Quantum Electronics*, vol. 48, no. 8, article 400, 2016.

[20] S. A. Aljunid, M. Ismail, A. R. Ramli, B. M. Ali, and M. K. Abdullah, "A new family of optical code sequences for spectral-amplitude-coding optical CDMA systems," *IEEE Photonics Technology Letters*, vol. 16, no. 10, pp. 2383–2385, 2004.